Rheol Acta 35:39–47 (1996)

ORIGINAL CONTRIBUTION

Georgios C. Georgiou

On the stability of the shear flow of a viscoelastic fluid with slip along the fixed wall

Received: 31 May 1995
Accepted: 6 October 1995

Prof. G.C. Georgiou (✉)
Department of Mathematics and Statistics
University of Cyprus
P.O. Box 537
1678 Nicosia, Cyprus

Abstract In this paper we solve the time-dependent shear flow of an Oldroyd-B fluid with slip along the fixed wall. We use a non-linear slip model relating the shear stress to the velocity at the wall and exhibiting a maximum and a minimum. We assume that the material parameters in the slip equation are such that multiple steady-state solutions do not exist. The stability of the steady-state solutions is investigated by means of a one-dimensional linear stability analysis and by numerical calculations. The instability regimes are always within or coincide with the negative-slope regime of the slip equation. As expected, the numerical results show that the instability regimes are much broader than those predicted by the linear stability analysis. Under our assumptions for the slip equation, the Newtonian solutions are stable everywhere. The interval of instability grows as one moves from the Newtonian to the upper-convected Maxwell model. Perturbing an unstable steady-state solution leads to periodic solutions. The amplitude and the period of the oscillations increase with elasticity.

Key words Shear flow – Oldroyd-B model – slip – linear stability analysis

Introduction

Slip at the wall and constitutive instabilities have been among the most popular explanations for extrusion instabilities of polymer melts. The reader is referred to the review paper of Larson (1992) for a detailed discussion. Convincing experimental evidence for the role of slip has been provided by various groups (Hill et al., 1990; Piau et al., 1990; Hatzikiriakos and Dealy, 1992). Empirical slip equations relating the shear stress to the velocity of the fluid at the wall have been proposed by El Kissi and Piau (1989), Leonov (1990) and Hatzikiriakos and Dealy (1992). One characteristic of the above slip equations is that in some range of slip velocities the slope of the shear stress/slip velocity curve is negative. The two-dimensional linear stability analysis for Newtonian Poiseuille flow shows that steady-state solutions in the negative-slope regime might be unstable (Pearson and Petri, 1965, 1968).

In a recent paper (Georgiou and Crochet, 1994), we studied the time-dependent compressible Newtonian Poiseuille flow with non-linear slip at the wall. Our numerical results show that when compressibility is taken into account and the volumetric flow rate at the inlet corresponds to the negative-slope regime of the slip equation, self-sustained oscillations of the pressure drop and of the mass flow rate at the exit are obtained. In the present work we show that the combination of non-linear slip and elasticity can also lead to self-sustained oscillations. To demonstrate this, we have chosen to study the shear flow of an Oldroyd-B fluid, a fluid with monotonic steady-shear response in the absence of slip. We assume that slip occurs along the fixed wall.

By choosing the Oldroyd-B model, we assure that the instabilities are caused by the non-linear slip equation whereas elasticity acts only as the storage of the elastic energy that sustains the oscillations. The present approach is thus fundamentally different from that of

Rheologica Acta, Vol. 35, No. 1 (1996)

various researchers who have considered models exhibiting a non-monotonic (i.e., double-valued) steady shear response (Yerushalmi et al., 1970; Lin, 1985; McLeish and Ball, 1986; Hunter and Slemrod, 1983; Kolkka et al., 1988; Malkus et al., 1989). One-dimensional linear stability analyses show that steady-state solutions are unstable whenever the slope of the shear stress-shear rate curve is negative. The presence of shear-stress maxima and minima results in an oscillatory motion of the fluid when some critical values are exceeded.

The governing equations and the boundary conditions for the time-dependent shear flow of an Oldroyd-B fluid with slip along the fixed wall are presented in the next section. Even though the linear stability analysis of the flow to two-dimensional disturbances is possible (Pearson and Petrie, 1968), it suffices, for our purposes, to carry out the much simpler one-dimensional linear stability analysis presented in the third section. We show that steady-state solutions corresponding to the negative-slope part of the slip equation might be unstable. Stability depends not only on the slope of the slip equation but also on the material parameters. The Newtonian solutions are always stable if the material parameters of the slip equation are such that the steady-state solutions are unique. The interval of instability grows as one moves from the Newtonian to the upper-convected Maxwell model. In the final section we present numerical results showing that the instability regimes are broader than those predicted by the linear stability analysis. Perturbing an unstable steady-state solution leads to periodic solutions. The amplitude and the period of the oscillations increase with elasticity.

Governing equations

We use the Oldroyd-B model for our studies. The extra stress tensor $\boldsymbol{T}$ is decomposed into a purely viscoelastic part $\boldsymbol{T}_1$ and a purely viscous part $\boldsymbol{T}_2$ (Crochet et al., 1984):

$$\boldsymbol{T} = \boldsymbol{T}_1 + \boldsymbol{T}_2 \ , \tag{1}$$

$$\boldsymbol{T}_1 + \lambda \overset{\nabla}{\boldsymbol{T}}_1 = 2\eta_1 \boldsymbol{d} \ , \tag{2}$$

$$\boldsymbol{T}_2 = 2\eta_2 \boldsymbol{d} \ . \tag{3}$$

In the above equations, η_1, η_2 and λ are material parameters. The shear viscosity is given by $\eta_1 + \eta_2$, and the ratio $\eta_2/(\eta_1+\eta_2)$ represents the ratio of the retardation time to the relaxation time. The Newtonian and the upper-convected Maxwell models are special cases of the Oldroyd-B model ($\eta_2 = 1$ and 0, respectively). Moreover, the symbol ∇ denotes the upper-convected derivative:

$$\overset{\nabla}{\boldsymbol{T}}_1 = \dot{\boldsymbol{T}}_1 - \nabla \boldsymbol{v} \cdot \boldsymbol{T}_1 - \boldsymbol{T}_1 \cdot (\nabla \boldsymbol{v})^T \ , \tag{4}$$

where $\dot{\boldsymbol{T}}_1$ is the time derivative of $\boldsymbol{T}_1$, $\boldsymbol{v}$ is the velocity vector, and the superscript T denotes the transpose. Finally, $\boldsymbol{d}$ is the rate-of-strain tensor defined by:

$$\boldsymbol{d} = \frac{1}{2}\left[(\nabla \boldsymbol{v}) + (\nabla \boldsymbol{v})^T\right] \ . \tag{5}$$

Let us now consider the time-dependent shear flow of an Oldroyd-B fluid. The geometry and the boundary conditions of the flow are shown in Fig. 1. The lower wall moves with velocity V_1. We assume that the fluid sticks to that wall and therefore:

$$v_x = V_1 \quad \text{at} \quad y = 0 \ . \tag{6}$$

The upper wall is fixed. We assume that slip occurs along this wall following a slip law of the general form:

$$\sigma_w = -F(v_w) \quad \text{at} \quad y = H \ , \tag{7}$$

where σ_w is the shear stress and v_w the velocity of the fluid at the wall (slip velocity). Note that considering the same flow with slip along the moving wall instead leads to a mathematically equivalent problem. (Considering slip along both walls leads to a flow with multiple steady-state solutions which is undesired in our study.)

The problem is one-dimensional $\left[\frac{\partial}{\partial x} = 0, v_x = v_x(y,t), v_y = 0 \text{ and } \boldsymbol{T}_1 = \boldsymbol{T}_1(y,t)\right]$, and the x-momentum equation is reduced to:

$$\rho \frac{\partial v_x}{\partial t} = \frac{\partial T^{xy}}{\partial y} = \frac{\partial T_1^{xy}}{\partial y} + \frac{\partial T_2^{xy}}{\partial y} \ , \tag{8}$$

where ρ is the density. The component T_1^{yy} is zero and remains so at all times (provided that the disturbances are one dimensional). For the other two components of $\boldsymbol{T}_1$ we have:

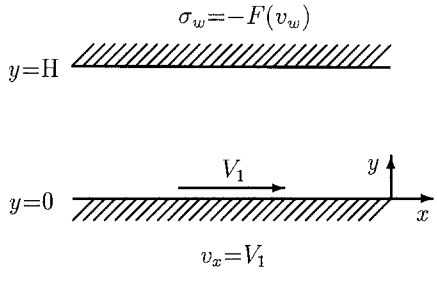

Fig. 1 Boundary conditions for the time-dependent shear flow with slip at the fixed wall

$$T_1^{xx}+\lambda\left(\frac{\partial T_1^{xx}}{\partial t}-2\frac{\partial v_x}{\partial y}T_1^{xy}\right)=0\ , \tag{9}$$

$$T_1^{xy}+\lambda\frac{\partial T_1^{xy}}{\partial t}=\eta_1\frac{\partial v_x}{\partial y}\ . \tag{10}$$

We observe that Eq. (9) for T_1^{xx} is not coupled with Eqs. (8) and (10), meaning that one can solve the system of the latter two equations first and then calculate T_1^{xx}.

We would like to work with the dimensionless equations. To non-dimensionalize the governing equations, we scale the lengths by the distance between the two walls H, the velocity by a characteristic velocity V, the stress components by $(\eta_1+\eta_2)V/H$, and the time by H/V. Equations (8) and (10) then become:

$$\mathrm{Re}\frac{\partial v_x}{\partial t}=\frac{\partial T_1^{xy}}{\partial y}+\frac{\partial T_2^{xy}}{\partial y}=\frac{\partial T_1^{xy}}{\partial y}+\eta_2\frac{\partial^2 v_x}{\partial y^2}\ , \tag{11}$$

$$T_1^{xy}+\mathrm{We}\frac{\partial T_1^{xy}}{\partial t}=\eta_1\frac{\partial v_x}{\partial y}\ . \tag{12}$$

All the variables in the above two equations are dimensionless, including η_1 and η_2 which are scaled by the shear viscosity; the dimensionless shear viscosity $\eta_1+\eta_2$ is thus equal to unity. Re and We are the Reynolds and Weissenberg numbers, respectively:

$$\mathrm{Re}\equiv\frac{\rho VH}{\eta_1+\eta_2}\ ;\quad \mathrm{We}\equiv\frac{\lambda V}{H}\ . \tag{13}$$

Analytical and approximate solutions

In this section, we provide the steady-state solutions of the system of (11) and (12) and then we study their stability to one-dimensional infinitesimal disturbances by means of a linear stability analysis. Moreover, we present some analytical results for the limiting case of zero Re.

Steady-state solution

The steady-state solutions are as follows:

$$v_x=V_1+(v_w-V_1)y\ , \tag{14}$$

$$T^{xy}=T_1^{xy}+T_2^{xy}=v_w-V_1\ , \tag{15}$$

where the slip velocity v_w satisfies the condition:

$$v_w-V_1=-F(v_w)\ . \tag{16}$$

In other words, v_x varies linearly with y and the shear stress is constant.

Let us now consider the slip equation used by Georgiou and Crochet (1994). This equation involves three material parameters, namely α_1, α_2 and α_3, and its dimensionless form is:

$$\sigma_w=-F(v_w)=-A_1\left(1+\frac{A_2}{1+A_3v_w^2}\right)v_w\ , \tag{17}$$

where

$$A_1\equiv\frac{\alpha_1 H}{\eta_1+\eta_2}\ ;\quad A_2\equiv\alpha_2\ ;\quad A_3\equiv\alpha_3V^2\ . \tag{18}$$

Equation (17) exhibits a maximum and a minimum of σ_w provided that $A_2>8$. Another constraint for the problem under study arises if we require that the velocity $V_1=v_w+F(v_w)$ be a monotonic function of v_w, i.e. we demand that the steady-state solutions be unique for a given value of V_1. This requirement is met in the general case when

$$F'(v_w)=\frac{dF(v_w)}{dv_w}>-1\ , \tag{19}$$

and in the case of Eq. (17) when

$$A_2<8\frac{1+A_1}{A_1}\ .$$

In Fig. 2, we show σ_w and V_1 as functions of v_w for $A_1=1$, $A_2=15$ and $A_3=100$.

Linear stability analysis

Let $(\bar{v}_x, \bar{T}_1^{xy})$ be a basic (i.e., steady-state) solution given by Eqs. (14) and (15). We will examine the transient response of the above basic solution to small one-dimensional perturbations $(v_x)^*$ and $(T_1^{xy})^*$:

$$v_x(y,t)=\bar{v}_x+(v_x)^*(y,t)\ , \tag{20}$$

$$T_1^{xy}(y,t)=\bar{T}_1^{xy}+(T_1^{xy})^*(y,t)\ , \tag{21}$$

with

$$(v_x)^*(y,t)=\hat{v}_x(y)e^{\kappa t}\ll\bar{v}_x\ , \tag{22}$$

$$(T_1^{xy})^*(y,t)=\hat{T}_1^{xy}(y)e^{\kappa t}\ll\bar{T}_1^{xy}\ . \tag{23}$$

The flow is considered linearly stable if $(v_x)^*$ and $(T_1^{xy})^*$ decay over a finite period of time, i.e., when κ is negative.

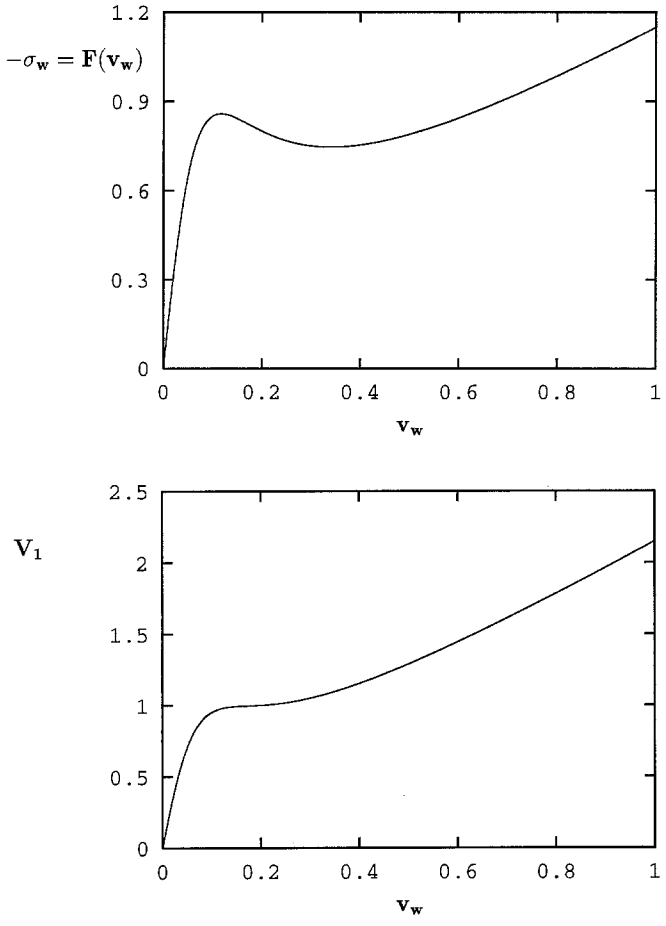

Fig. 2 a) Shear stress σ_w as a function of v_w with Eq. (17). b) Velocity V_1 of the lower wall as a function of v_w (steady-state solution). $A_1 = 1$, $A_2 = 15$ and $A_3 = 100$

In the case where the above quantities grow or oscillate with an undamped amplitude the flow is considered unstable.

Substituting Eqs. (20)–(23) in the governing Eqs. (11) and (12) gives:

$$\mathrm{Re}\,\kappa\,\hat{v}_x = \frac{d\hat{T}_1^{xy}}{dy} + \eta_2 \frac{d^2\hat{v}_x}{dy^2} \ , \tag{24}$$

$$\hat{T}_1^{xy} = \frac{\eta_1}{1+\mathrm{We}\,\kappa}\frac{d\hat{v}_x}{dy} \ . \tag{25}$$

Combining Eqs. (24) and (25) leads to the following ODE:

$$\frac{d^2\hat{v}_x}{dy^2} - \frac{\mathrm{Re}\,\kappa\,(1+\mathrm{We}\,\kappa)}{1+\eta_2\,\mathrm{We}\,\kappa}\hat{v}_x = 0 \ . \tag{26}$$

The linearized boundary conditions read:

$$\hat{v}_x = 0 \ , \quad \text{at } y = 0 \ , \tag{27}$$

$$\left(\frac{1+\eta_2\,\mathrm{We}\,\kappa}{1+\mathrm{We}\,\kappa}\right)\frac{d\hat{v}_x}{dy} = -F'(\bar{v}_w)\,\hat{v}_x \ , \quad \text{at } y = 1 \ , \tag{28}$$

where $F'(\bar{v}_w)$ is the derivative of F.

Solving the system of the linearized equations yields the following expression for $(v_x)^*$:

$$(v_x)^*(y,t) = \sum_{n=2}^{\infty} \alpha_n e^{\kappa_n t}\sin(m_n y) + \alpha_0 e^{\kappa_0 t}\sinh(m_0 y) + \alpha_1 e^{\kappa_1 t}\sinh(m_1 y) \ . \tag{29}$$

There are thus two fundamental solution sets, the forms of which are dictated by the boundary conditions. The coefficients α are determined on the basis of the initial conditions.

The eigenvalues m_n, $n = 2, 3, \ldots$ are the positive zeroes of

$$\mathrm{Re}\,\kappa\frac{\cot m}{m} = F'(\bar{v}_w) \ , \tag{30}$$

with

$$\kappa = -\frac{1}{2\,\mathrm{We}}\left[1+\eta_2\left(\frac{\mathrm{We}}{\mathrm{Re}}\right)m^2 \pm \sqrt{\left\{1+\eta_2\left(\frac{\mathrm{We}}{\mathrm{Re}}\right)m^2\right\}^2 - 4\left(\frac{\mathrm{We}}{\mathrm{Re}}\right)m^2}\right] \ . \tag{31}$$

Given that $\kappa_n < 0$, all the terms of the first fundamental solution set will decay.

The eigenvalues m_0 and m_1 are the positive roots of

$$\mathrm{Re}\,\kappa\frac{\coth m}{m} = -F'(\bar{v}_w) \ . \tag{32}$$

If $F'(\bar{v}_w) > 0$, it can be shown that Eq. (32) has a unique solution with

$$\kappa_0 = -\frac{1}{2\,\mathrm{We}}\left[1-\eta_2\left(\frac{\mathrm{We}}{\mathrm{Re}}\right)m^2 + \sqrt{\left\{1-\eta_2\left(\frac{\mathrm{We}}{\mathrm{Re}}\right)m^2\right\}^2 + 4\left(\frac{\mathrm{We}}{\mathrm{Re}}\right)m^2}\right] \ ; \tag{33}$$

in other words, the m_1 term drops out. Because $\kappa_0 < 0$, the relevant term decays and the basic solution is stable.

If, however, $-1<F'(\bar{v}_w)<0$, then there might be two or one or no solutions of Eq. (32) with

$$\kappa=\frac{1}{2\,\mathrm{We}}\left[-1+\eta_2\left(\frac{\mathrm{We}}{\mathrm{Re}}\right)m^2+\sqrt{\left\{1-\eta_2\left(\frac{\mathrm{We}}{\mathrm{Re}}\right)m^2\right\}^2+4\left(\frac{\mathrm{We}}{\mathrm{Re}}\right)m^2}\right], \quad (34)$$

depending on the value of $F'(\bar{v}_w)$ and the ratio (We/Re). If a solution does exist, then the initial disturbances will grow because κ is positive.

In Fig. 3, we show the stability curves for various values of η_2. For a given η_2, the stability of a basic solution is determined from the values of $F'(\bar{v}_w)$ and (We/Re). If $F'(\bar{v}_w)>0$, the solution is stable independently of the value of (We/Re). If $F'(\bar{v}_w)<0$, the solution is unstable if

$$-1<-F'(\bar{v}_w)<S_{\mathrm{crit}}<0\ ,$$

where S_{crit} is an increasing function of (We/Re). Note that $F'(\bar{v}_w)$ cannot be less than -1 due to our assumption that V_1 is a monotonic function of v_w in steady state. We observe that increasing the value of η_2 reduces the size of the instability regime. The Newtonian flow [(We/Re) = 0 or $\eta_2 = 1$] is always stable.

In the limit of zero Reynolds number [(We/Re)$\to\infty$], it is easily shown that the shear stress components, T_1^{xy} and T_2^{xy}, remain constant and the velocity v_x remains linear at all times. Applying the conditions (27–28) explicitly gives the value of κ:

$$\kappa=-\frac{1+F'(\bar{v}_w)}{\mathrm{We}\,[\eta_2+F'(\bar{v}_w)]}\ . \quad (35)$$

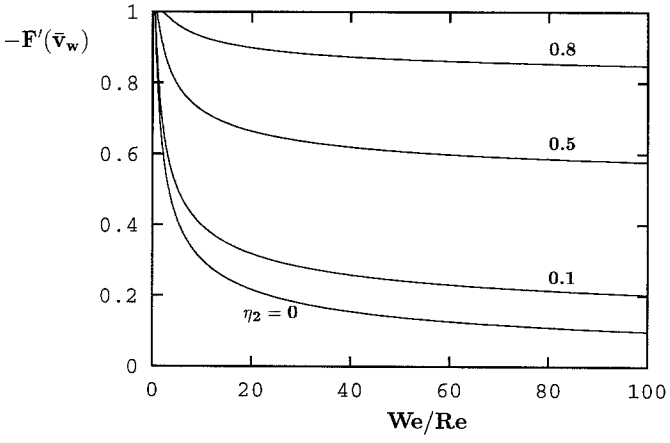

Fig. 3 Stability curves for the shear flow of an Oldroyd-B fluid with slip along the fixed wall. The flow is unstable above the corresponding curve. The curves go to η_2 as (We/Re)$\to\infty$

Given that $F'(\bar{v}_w)>-1$, the steady-state solutions are unstable when

$$-1<F'(\bar{v}_w)<-\eta_2\ . \quad (36)$$

The stability curves of Fig. 3 asymptotically approach the value η_2.

Results for Re = 0

For Re = 0, the validity of the linear-stability results is not restricted to infinitesimal disturbances. It is easily shown that for Re = 0, T_1^{xy} is independent of y and v_x varies linearly with y at all times:

$$T_1^{xy}(y,t)=-F(v_w)-\eta_2(v_w-V_1)\ . \quad (37)$$

$$v_x(y,t)=V_1+(v_w-V_1)y\ , \quad (38)$$

where the slip velocity v_w satisfies the following ODE:

$$\mathrm{We}\,[F'(v_w)+\eta_2]\frac{dv_w}{dt}+v_w+F(v_w)=V_1\ . \quad (39)$$

If we perturb $\bar{v}_w$ to v_w^0 and assume that the derivative $F'(v_w)$ is locally constant, Eq. (39) gives:

$$v_w=\bar{v}_w+(v_w^0-\bar{v}_w)\exp\left\{-\frac{1+F'(\bar{v}_w)}{\mathrm{We}\,[\eta_2+F'(\bar{v}_w)]}t\right\}\ . \quad (40)$$

One can observe that the derivative term of Eq. (39) vanishes at the points where

$$F'(v_w)=-\eta_2\ . \quad (41)$$

These points are obviously limit points: if v_w reaches such a point it will stay there and will never reach the steady-state corresponding to the imposed value of V_1. In the case of the Maxwell fluid ($\eta_2 = 0$), the limit points are the extrema of $F(v_w)$. If Re = 0 and the function $F(v_w)$ is twice differentiable and exhibits a maximum at $v_w^{\max}$ and a minimum at $v_w^{\min}$, as in Eq. (17), meaning that its slope is negative and continuous in the open interval $(v_w^{\max}, v_w^{\min})$, there exist two possibilities:

1) $-\eta_2<F'(v_w)<0$.
The flow is stable for all values of v_w. This possibility does not obtain with the Maxwell fluid ($\eta_2 = 0$).
2) $-1<F'(v_w)<0$ and $F'(v_w)=-\eta_2$ at v_w^{L1} and v_w^{L2}, where $v_w^{L1}<v_w^{L2}$.
The points v_w^{L1} and v_w^{L2} are obviously limit points. The solution is unstable in (v_w^{L1}, v_w^{L2}). This case is illustrated in Fig. 4. Due to the presence of the two limit

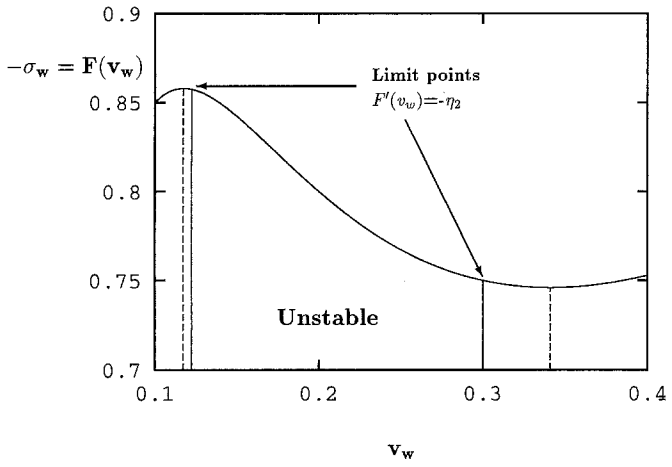

Fig. 4 Interval of instability and limit points for Re = 0

points, the steady solution on one stable branch cannot be reached if $v_w(t = 0)$ is on the other branch.

Numerical results

We use standard finite elements in space and a fully-implicit (Euler backward difference) scheme in time for the numerical solution of the system of Eqs. (11) and (12). The method has been tested against the predictions of Eq. (40) in the case of a linear slip equation. Excellent agreement has been found. In all subsequent results we use the slip Eq. (17) with $A_1 = 1$, $A_2 = 15$ and $A_3 = 100$. Recall that in our time-dependent runs we start from a steady-state solution (v_w^0, V_1^0) and perturb V_1^0 to V_1 at $t = 0$.

We first verify the findings of the analysis of the previous section for Re = 0. Let us consider two different values of η_2: 0.9 and 0.1. When $\eta_2 = 0.9$, the steady-state solutions are stable everywhere because $F'(\bar{v}_w) > -\eta_2$ for all $\bar{v}_w$; the solution always converges to the new steady state, even when V_1 corresponds to the negative-slope regime of the slip equation. In Fig. 5a, we illustrate the evolution of v_w when $V_1^0 = 0.6$, $V_1 = 1.01$ $(F'(\bar{v}_w) = -0.6)$, and We = 1. Notice that v_w initially jumps towards the new steady state, an effect not visible in Fig. 5a.

If now $\eta_2 = 0.1$, then the flow is unstable in the subinterval of the negative-slope regime of the slip equation where $F'(v_w) < -\eta_2$. Let us again take $V_1 = 1.01$ and We = 1. In Fig. 5b, we summarize all the different possibilities when V_1 falls into the unstable regime: a) If V_1^0 corresponds to one of the two stable branches of the slip equation, then v_w initially appears to approach the unstable steady state but stops when it reaches the nearest limit point. b) If V_1^0 corresponds to the unstable branch

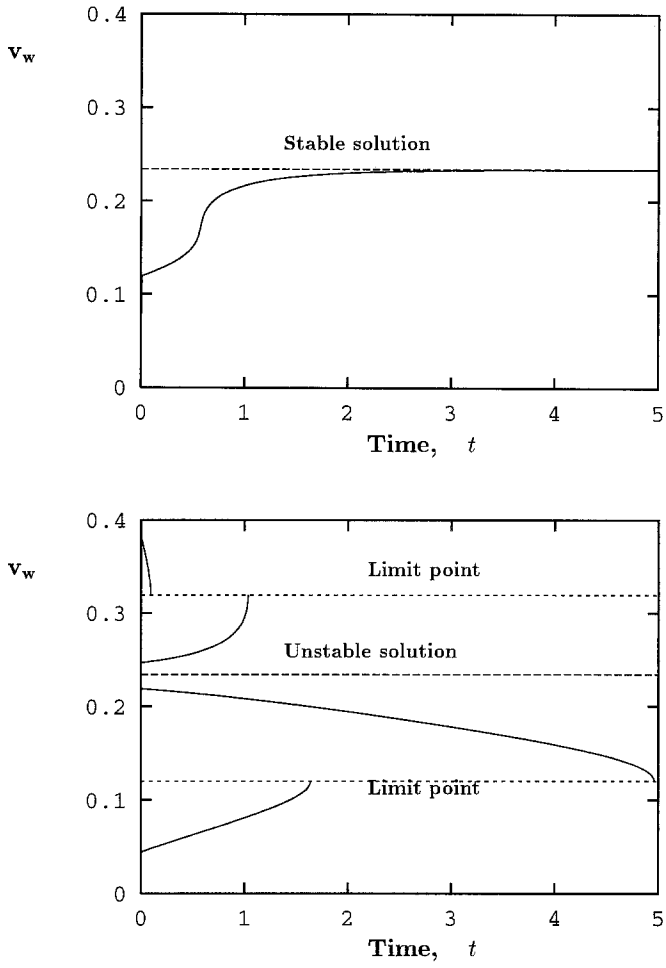

Fig. 5 a) Convergence of v_w to a stable solution in the negative-slope regime of the slip equation ($\eta_2 = 0.9$). b) Evolution of v_w from different initial states when V_1 corresponds to an unstable solution ($\eta_2 = 0.1$). $V_1 = 1.01$, We = 1 and Re = 0

of the slip equation, then v_w moves away from the unstable steady state and hits one of the limit points.

The numerical calculations for non-zero Reynolds numbers show that the instability regimes are broader than those predicted by the linear stability analysis. This, of course, is expected because linear stability analyses are valid only for infinitesimal disturbances. Let us consider again the basic solution for $V_1 = 1.01$ $(F'(\bar{v}_w) = -0.6)$, Re = 0.01 and $\eta_2 = 0.1$. According to the linear stability analysis the flow is unstable for We greater than 0.0298 (Fig. 3). Our calculations show that the critical value of We at which instability appears is much lower (~ 0.009) and decreases even further as the size of the perturbation increases. Our calculations show that above this critical value the solution becomes periodic irrespective of the initial conditions and that the amplitude and the period of the oscillations only depend on the imposed value of V_1.

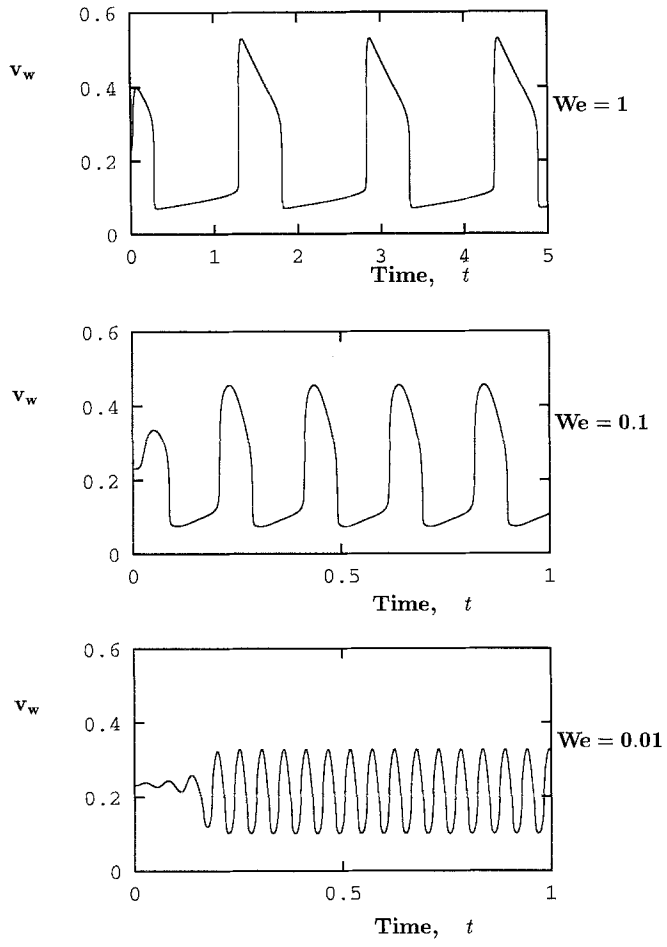

Fig. 6 Periodic solutions for different values of We when V_1 is in the unstable regime; $V_1^0 = 1.009$, $V_1 = 1.01$, $\eta_2 = 0.1$ and Re = 0.01

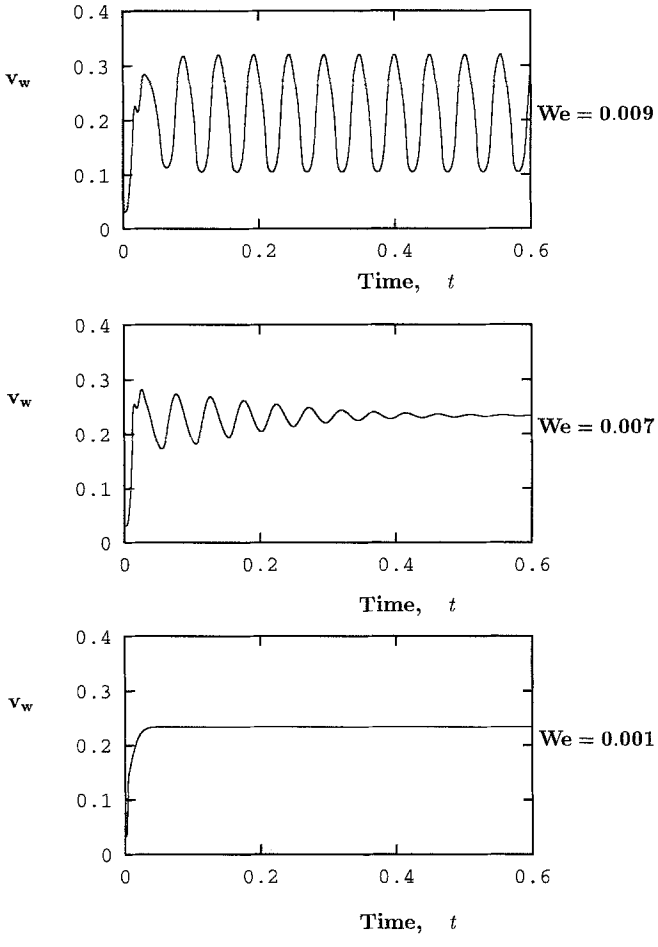

Fig. 7 Solutions for small values of We when V_1 is in the unstable regime; $V_1^0 = 0.5$, $V_1 = 1.01$, $\eta_2 = 0.1$ and Re = 0.01

In Fig. 6, we illustrate the effect of the We on the amplitude and the period of the oscillations of the slip velocity v_w. The imposed value of V_1 is 0.01 and we start from the steady-state solution at $V_1^0 = 1.009$ (i.e., the perturbation is "small"). The amplitude and the period of the oscillations increase with elasticity. Below a critical value of the Weissenberg number (~ 0.009) the flow becomes stable. If we increase the size of the perturbation, however, this critical Weissenberg number is even more reduced. This is shown in Fig. 7, where we start from $V_1^0 = 0.5$. In Fig. 8, we plot the amplitude (Δv_w) and the period (T_p) of the slip velocity oscillations vs We.

Finally, in Fig. 9, we show the effect of the viscosity scale η_s. Increasing η_s affects only the values of Re and A_1 which are inversely proportional to η_s. This is equivalent to reducing the "real" Reynolds number. As expected, the amplitude and the period of the oscillations are reduced as we increase η_s and below a critical value of the flow becomes stable.

Conclusions

We have studied the time-dependent shear flow of an Oldroyd-B fluid considering non-linear slip along the fixed wall. According to the one-dimensional linear stability analysis, the Newtonian solutions are always stable, under our assumptions for the slip equation parameters. The instability regimes, which are always within or coincide with the negative-slope regime of the slip equation, grow in size as one moves from the Newtonian to the upper-convected Maxwell model. The numerical calculations show that the instability regimes are much broader than those predicted by the linear stability analysis, their size depending on the magnitude of the perturbation. The combination of non-linear slip and elasticity results in periodic solutions in the unstable regime. The amplitude and the period of the oscillations increase with elasticity.

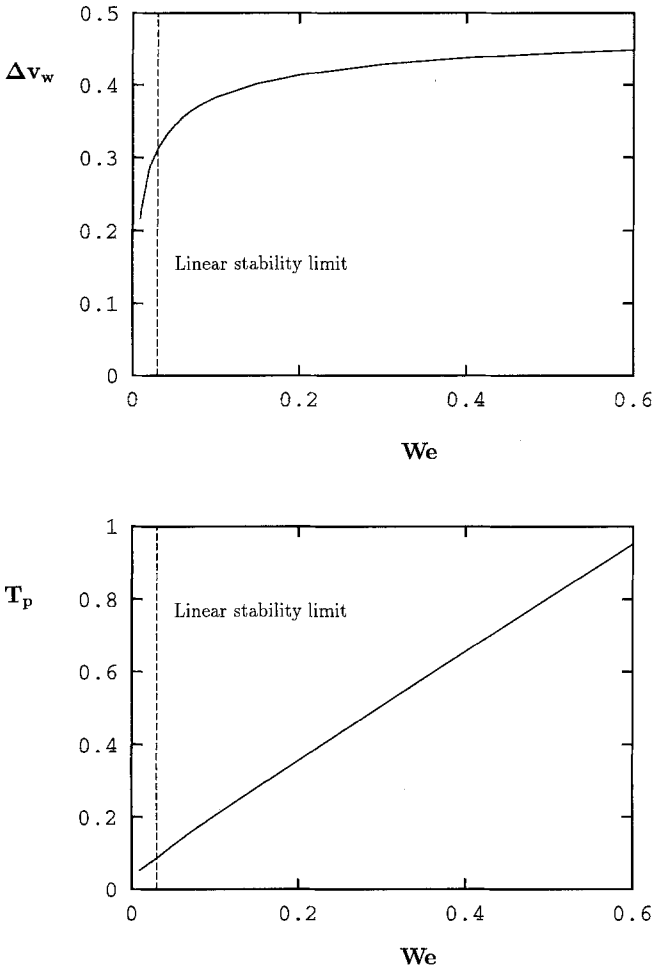

Fig. 8 Amplitude Δv_w and period T_p of the oscillations of v_w; Re = 0.01, $\eta_2 = 0.1$ and $V_1 = 1.01$

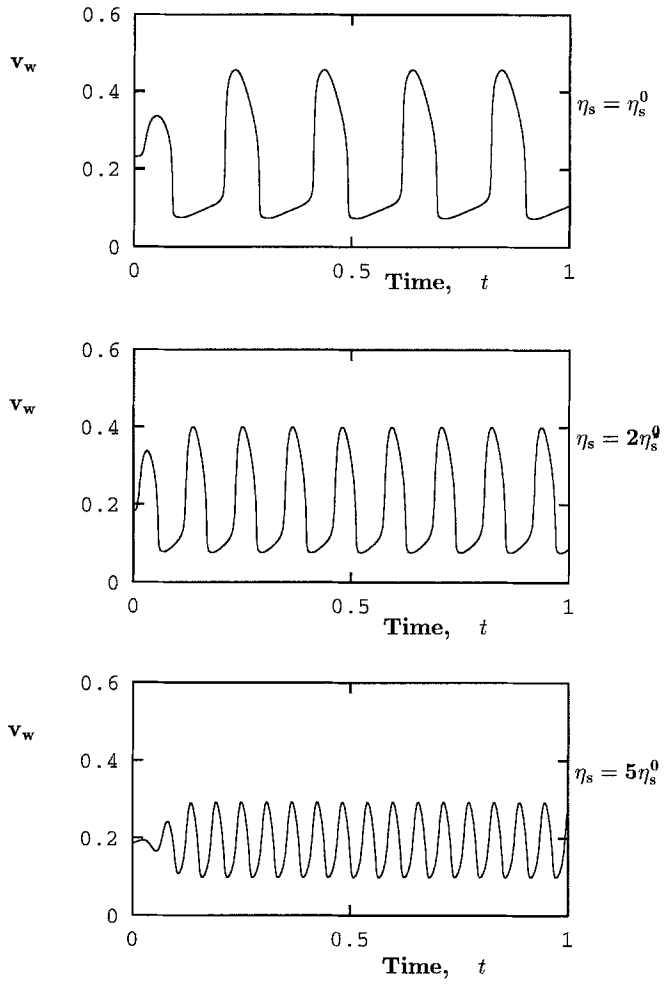

Fig. 9 Effect of the viscosity scale η_s; $V_1 = 1.01$, $\eta_2 = 0.1$, We = 0.1 and Re = 0.01

Acknowledgements The author is grateful for the support, hospitality and helpful discussions of Prof. Marcel Crochet of Unité de Mécanique Appliquée, Université Catholique de Louvain, from which this work evolved. This paper presents research results of the Belgian Programme on Interuniversity Poles of Attraction, initiated by the Belgian State, Prime Minister's Office for Science, Technology and Culture. The scientific responsibility rests with its author. The paper is dedicated to the memory of Prof. Tasos Papanastasiou.

References

Crochet MJ, Davies AR, Walters K (1984) Numerical simulation of non-Newtonian flow. Elsevier Science Publishers

El Kissi N, Piau JM (1989) Ecoulement de fluides polymères enchevêtrés dans un capillaire. Modélisation du glissement macroscopique à la paroi. CR Acad Sci Paris t. 309, Série II:7–9

Georgiou GC, Crochet MJ (1994) Compressible viscous flow in slits, with slip at the wall. J Rheology 38:639–654

Hatzikiriakos SG, Dealy JM (1992a) Wall slip of molten high density polyethylenes. II. Capillary rheometer studies. J Rheol 36:703–741

Hatzikiriakos SG, Dealy JM (1992b) Role of slip and fracture in the oscillating flow of HDPE in a capillary. J Rheol 36:845–884

Hill DA, Hasegawa T, Denn MM (1990) On the apparent relation between adhesive failure and melt fracture. J Rheology 34:891–918

Hunter JK, Slemrod M (1983) Viscoelastic fluid flow exhibiting hysteritic phase changes. Phys Fluids 26:2345–2351

Kolkka RW, Malkus DS, Hansen MG, Ierley GR, Worthing RA (1988) Spurt phenomena of the Johnson-Segalman fluid and related models. J Non-Newtonian Fluid Mech 29:303–335

Larson RG (1992) Instabilities in viscoelastic flows. Rheol Acta 31:213–263

Leonov AI (1990) On the dependence of friction force on sliding velocity in the theory of adhesive friction of elastomer. Wear 141:137–145

Lin Y-H (1985) Explanation for stick-slip melt fracture in terms of molecular dynamics in polymer melts. J Rheol 29:605–637

McLeish TCB, Ball RC (1986) A molecular approach to the spurt effect in polymer melt flow. J Polym Sci B24:1735–1745

Pearson JRA, Petrie CJS (1965) On the melt-flow instability of extruded polymers. Proc. 4th Int. Rheological Congress 3:265–282

Pearson JRA, Petrie CJS (1968) On melt flow instability of extruded polymers. In: Wetton RE, Whorlow RW (eds) Polymer systems: deformation and flow. Macmillan, London 163–187

Piau JM, El Kissi N, Tremblay B (1990) Influence of upstream instabilities and wall slip on melt fracture and sharkskin phenomena during silicones extrusion through orifice dies. J Non-Newtonian Fluid Mech 34:145–180

Yerushalmi J, Katz S, Shinnar R (1970) The stability of steady shear flows of some viscoelastic fluids. Chem Eng Sci 25:1891–1902